Ticagrelor-Pretreated Cardiomyocyte Derived Exosomes Provide Cardioprotection Under Hyperglycemia Through Alleviation In Oxidative Stress, Apoptosis, And ER-Stress

Ceylan Verda Bitirim
Ankara University
Zeynep Busra Ozer
Ankara University
Dunya Aydos
Ankara University
Kardelen Genc
Ankara University
Seyma Demirsoy
Pennsylvania State University
Kamil Can Akcali
Ankara University
Belma Turan (belma.turan@medicine.ankara.edu.tr)
Ankara University

Research Article

Keywords: diabetes, exosomes, P2Y12-receptors, autophagy, apoptosis, ER-stress, heart.

Posted Date: October 25th, 2021

DOI: https://doi.org/10.21203/rs.3.rs-958741/v1

Abstract

Exosomes play important roles in Diabetes Mellitus (DM) via connecting the immune cell response to tissue injury, besides stimulation to muscle insulin resistance, while DM is associated with increase risks for major cardiovascular complications. Under DM, chronic hyperglycemia and subsequent augmentation of reactive oxygen species (ROS) further lead to cardiac growth remodeling and dysfunction. Although a P2Y12 receptor inhibitor, ticagrelor, is widely used in cardioprotection, its inhibitory effect on diabetic cardiomyopathy is poorly elucidated. Here, we aimed to investigate the anti-oxidative and cardioprotective effect of exosomes, derived from ticagrelor pretreated-cardiomyocytes. To mimic DM in cardiomyocytes, we used high glucose incubated H9c2-cells (HG). HG cells were treated with exosomes, which were derived from either ticagrelor-pretreated or untreated H9c2-cells. Our results demonstrated that exosomes derived from ticagrelor-pretreated H9c2-cells significantly decreased the aberrant ROS production, prevented the development of apoptosis and ER stress under hyperglycemia, and alleviated oxidative stress associated with a miRNA-expression profile. Importantly, exosomes derived from ticagrelor-pretreated H9c2-cells enhanced endothelial cell migration and tube formation, suggesting a modulation of the exosome profile in cardiomyocytes. Our data, for the first time, indicate that ticagrelor can exert an important regulatory effect on diabetic cardiomyopathy through exosomal modulation behind its receptor-inhibitor related action.

Introduction

Diabetes mellitus (DM) is a complex disease caused by a complex interplay between genetic, epigenetic, and environmental factors and characterized by metabolic abnormalities, as well. It is well-known that DM causes a variety of micro-, and macro-vascular complications such as cardiomyopathy, atherosclerosis, and coronary heart disease [1]. In diabetic patients, heart failure develops not only because of the underlying coronary artery disease but also because of the multiple pathophysiological and metabolic abnormalities induced by altered glucose metabolism [2]. Primary and secondary prevention of cardiovascular disease (CVD) involves a multifactorial approach to treat the cluster of risk factors including hyperglycemia, hypercoagulation, and hypertension. The clinical outcomes emphasized that the altered systemic and cardiac glucose metabolism directly contributes to cardiac contractility and function in DM patients thereby triggering ventricular dysfunction [3]. The alteration of cardiac function in diabetics occurs through the activation and/or deactivation of several signaling pathways. Those specific signaling pathways play pivotal roles in the regulation of angiogenesis, production of reactive oxygen species (ROS) which are compromising the myocardial contractility, mitochondrial function/structure, oxidative stress, and cellular death mechanisms such as apoptosis and autophagy [4–7]. Therefore, elucidating the mechanisms of cardiometabolic drug actions on these complex signaling pathways is critical to support novel clinical indications.

Ticagrelor is the most successful purinergic drug, which reversibly targets ADP-mediated G protein-coupled (GPCR) purinergic receptor P_2Y_{12}, [5,6] and has been widely used in patients with acute coronary

syndrome (ACS) and myocardial infarction (MI). Several clinical studies have reported the higher efficacy and lower risk of ticagrelor application in ischemic events such as cardiovascular and coronary heart diseases comparing to clopidogrel that is a P_2Y_{12} receptor antagonist and irreversibly blocks P_2Y_{12} [1,7].

Cardioprotective and therapeutic potential of the extracellular vesicles (EV), such as microvesicles and exosomes, is presenting a promising and alternative treatment in cardiovascular diseases [8]. In the last decade, it was indicated that cardiovascular cells, such as cardiomyocytes, endotheliocytes, fibroblasts, platelets, smooth muscle cells (SMCs) -derived exosomes play critical roles in mediating inflammatory and coagulative reactions [9], neovascularizations, and cell migration [10,11] in patients with stable coronary artery disease (CAD) and atherosclerosis. Supporting, previous studies implied the important role of stem cells and exosomes in cardiac repair through demonstration of inhibited apoptosis in hyperglycemic cardiomyoblasts by exosomes derived from cardiac parasympathetic ganglionic neurons inhibit [12] as well as through shown impact of high glucose on mesangial cell-derived exosome composition, secretion and cell communication [13]. However, how the conventional cardiovascular drugs modulate cardiovascular cell-derived exosomes and how secreted exosomes exert their cardioprotective effect has not been investigated in detail yet. Furthermore, ticagrelor, a P_2Y_{12} receptor antagonist, beyond receptor inhibition, provides pleiotropic effects under different pathological conditions, including both in vitro and in vivo studies [14,15]. For instance, Casieri and co-workers showed the important benefit of exosomes derived from pre-treated human cardiac progenitor cell (h-CPC) hypoxia-induced apoptosis [16]. In another study, it has been demonstrated amelioration of DM effects in mesenchymal stem cell-derived exosomes by improving hepatic glucose and lipid metabolism via enhancing autophagy [17]. In addition, the direct effect of ticagrelor on mitochondrial dysfunction through suppressing ER stress and markedly decreasing autophagosome-dependent apoptosis in insulin-resistant H9c2 myocytes, expressed P_2Y_{12} receptors, was also reported [18].

Therefore, taken into consideration the cardio-regulatory effects of ticagrelor contributing to the exosome modulation and preventing the insulin-resistant cardiomyocytes against ER stress and induced apoptosis, in this study, we investigated the anti-oxidative and cardioprotective role of ticagrelor pre-treated cardiomyocytes-derived exosomes on hyperglycemic cardiomyocytes. For this aim, we have mimiced the DM model by treating the H9c2 cells with high glucose (25-mM). We hypothesized that ticagrelor treatment modulates the exosomes released from H9c2 cells via reducing hyperglycemia associated with enhanced ROS production, ER stress, and autophagy. Investigating the modulatory mechanism of ticagrelor as a widely-used cardiovascular drug may improve the beneficial use in terms of administration in antiplatelet treatment strategies.

Materials And Methods

Cell culture

The H9c2 cell line was derived from the left ventricle of the embryonic rat heart (CRL1446) and Primary Human Umbilical Vein Endothelial Cells (HUVEC) derived from the vein of the umbilical cord (CRL1730) were purchased from The American Type Culture Collection. H9c2 cells and HUVEC were grown in modified Dulbecco's modified Eagle's medium (DMEM) including 5.5 mM glucose (low glucose) and DMEM/F12 medium, respectively. Both media includes 10% fetal calf serum (F2442, Sigma-Aldrich, USA), 50 U/mL penicillin-G, and 50 µg/mL streptomycin. To obtain hyperglycemic cells, H9c2 cells were incubated with DMEM, including 25 mM glucose instead of 5.5 mM (HG-group). Before the exosome isolation, one group of H9c2 cells were incubated with ticagrelor (1-µM) for 72-hours [18,49]. The cells incubated with only the FBS medium were kept as control (Control-group). At the end of this period, exosomes were isolated from both control (untreated) and ticagrelor-treated H9c2 cells.

HG-H9c2 cells were treated with 0.5 ug exosome isolated from either control (+Exo) or ticagrelor treated H9c2 cells (Tica-Exo) for 48 hours. The experimental protocol followed step by step was given in Figure1.

Exosome Isolation

Exosomes were isolated from the supernatant using qEV T Size exclusion chromatography (SEC) columns (İzon Science, Poland) according to the manufacturer's protocol. Briefly, the collected supernatant either from ticagrelor-treated and control H9c2 cells was centrifuged at 10,000xg for 10 minutes and the supernatant was added into columns. The particles were separated and purified optimum between at 35 nm and 350 nm range. The collected particle suspension was centrifuged at 100,000xg for 1-h to increase the concentration.

Exosome Characterization And Quantification

Exosome characterization was performed by flow cytometric analysis. The exosomes were incubated with magnetic beads coated with anti-human CD9 antibody (Biolegend, SanDiego, Cat no: 312102). The exosome-magnetic bead mixture was detected by PE-conjugated anti-human CD81 antibody (Biolegend, SanDiego, Cat no: 104905). The size distribution and quantification of isolated exosomes were also measured using qNanoGold (Izon Science, Poland). For exosome samples, a polyurethane nanopore rated for particles <100 nm (NP100-, Izon Science, UK) was used. The concentration of exosomes was evaluated by Micro BCA assay (Thermo Fisher). Internalization of exosomes to H9c2 cells was also validated by confocal microscopy. The cells were treated with DiI labeled exosomes and visualized by confocal microscopy (Zeiss)

Wound Healing Assay

Endothelial cell migration was evaluated by the scratch assay, as previously reported [50]. Briefly, a total of 1×10^5 HUVECs were seeded -in full endothelial growth medium- in 6-well plates and allowed to form a

monolayer overnight at 37°C in a 5% CO_2 incubator. Using a p200 pipette tip, scratches were made in each well of the confluent monolayer. The medium was changed and the cells were treated with either 0.5 µg exosomes derived from control or ticagrelor treated H9c2 cells. The wound closure was visualized at 6 h, 48 h, and 72 h of incubation by an inverted light microscope (Zeiss). Migration was quantified by measuring the width of the cell-free zone by wound healing Analyzer plug-in for ImageJ (NIH, USA) [51]. The changes in the migration of exosome-treated cells were expressed comparing to (untreated) controls as the pixel. Values represent the mean (± SD) of triplicate scratches.

Tube Formation Assay

Tube formation assay was performed by the scratch assay, as previously reported [52]. Briefly, a total of 35×10^4 HUVECs were seeded in Matrigel-coated (Corning, USA) 96-well plates in DMEM-F12 including 1% exo-free FBS. The cells were treated with either 0.5 µg exosomes derived from control or ticagrelor treated H9c2 cells. The tube formation was visualized at 6 h and 24 h of incubation by an inverted light microscope (Zeiss). Branche, mesh, segment, and node formations were analyzed by Angiogenesis Analyzer plug-in for ImageJ (NIH, USA) [53]. Changes in angiogenesis on exosome-treated cells were expressed as a percentage of the controls (untreated cells). Values represent the mean (±SD) of triplicate formation assay.

Ros Measurements By Confocal Microscopy

Cells are loaded with 10-µM DCDFA probe (Cat no: D6883), ROS indicator chloromethyl-2',7'-dichlorodihydrofluoroscein diacetate, by incubating cells for 60-min at room temperature. Probe-loaded cells are scanned by a confocal microscope (Leica TCS SP5) at ~490–520 nm since record response to HEPES-buffered solution supplemented with 100-µM H_2O_2. The fluorescence intensity changes for every cell are calculated by $\Delta F/F0$, where $\Delta F = F - F0$; F is identified as local maximum elevation of fluorescence intensity over basal level, $F0$.

The measurement of mRNA levels of cellular and exosomal miRNAs by qRT-PCR

To analyze mRNA levels of cellular miRNAs, total RNA of H9c2 cardiomyocytes was isolated by using RiboEx Reagent (GeneAll, Korea) and the purified total-RNA was reverse transcribed with Entlink cDNA Synthesis-kit (Elk Biotech.,Wuhan), as described previously [54]. MicroRNA isolation from exosomes was performed using the total exosomal RNA isolation kit (Thermo Fischer; Cat no: 4478545). For miRNA qRT-PCR, stem-loop RT primers, that were designed for each miRNA, were used for cDNA Synthesis [55]. Shortly, GoTaq® qPCR Master Mix (Promega, A6001) was used to quantify and amplified PCR products for each primer, and primers' specificity was controlled with known databases. The fold changes of genes were analyzed based on the comparative ($2 - \Delta\Delta Ct$) method. For miRNA-qPCR, the universal reverse primer sequence; 5'-CCA GTG CAG GGT CCG AGG TA-3' was used as antisense [56]. The primers designed for qRT-

PCR are given in Supplementary Table 1, and stem-loop RT primers and forward primers designed for each miRNA are given in Supplementary Table 2.

Identification of differentially expressed miRNAs from public microarray data

To identify the differentially expressed miRNAs (DEMIs) significantly related to diabetic cardiomyopathy, the miRNA expression profile GSE44179 based on GPL14613 (miRNA-2_0) Affymetrix Multispecies miRNA-2_0 array was downloaded from the Gene Expression Omnibus (GEO) database (http://www.ncbi.nlm.nih.gov/geo/). The samples contained in GSE44179 were left ventricle (LV) myocardial tissues from a high-fat diet and streptozotocin (STZ)-induced diabetic (n=4) and non-diabetic control (n=2) Wistar rats (Raut, 2015). Then, DEMIs between diabetic and control samples were screened out via the GEOquery (Davis, 2007) and limma packages of R in which the expression data was fit to a linear model after filtering lowly-expressed genes with median expression level as a threshold and assigning relative quality weights for each sample [57]. The cut of criteria was set as adjusted p-value< 0.05 and |logFC|>1. To further visualize the results of differential expression analysis, the heat map of hierarchical clustering based on Euclidean distance with complete linkage metric and volcano plot were constructed using the R packages pheatmap [58]; ggplot2 [59] and ggrepel [60], respectively.

The potential target genes of DEMIs were predicted through TargetScan v7.2 (http://www.targetscan.org/vert_72/)[61] and miRDB (http://mirdb.org)[62] integrated into the miRWalk v2.0 (http://mirwalk.umm.uni-heidelberg.de/) predicted target module [63] and then screened by Venn diagram to find out the common targets with those of rat miR-499-5p, miR-133a-5p, miR-133b-5p, which were identified by DIANA- micro T-CDS v5.0 with the miRNA target gene (miTG) prediction score threshold of 0.7 (http://www.microrna.gr/microT-CDS/)[64]. A regulatory network of miR-499-5p, miR-133a-5p, miR-133b-5p associated to those common targets were constructed using Cytoscape v3.8.2 (https://cytoscape.org). Gene Ontology (GO) and KEGG pathway enrichment of the predicted interactions were performed using the functional analysis mode of the Cytoscape plugin ClueGO v2.5.7 [65]. The statistical significance of each term and pathway analyzed was calculated with a two-sided hypergeometric test and Bonferroni step-down *p*-value correction and a predefined kappa score level (≥0.4) was set to link them for a functionally grouped network (only annotations with the significance selection criteria as $p \leq 0.05$ were shown). Raw data of GO-enriched functional annotations for the predicted targets of miR-499, miR-133a, and miR-133b given as Supplementary file.

Statistical analysis

All data are expressed as ± standard deviation (± SD). Statistical comparisons were made by analysis of variance (ANOVA) and t-test. A value of p <0.05 was considered statistically significant. Analysis was performed using GraphPad PRISM software (GraphPad Software Inc., San Diego, California).

Results

Characterization and the levels of particles H9c2-derived exosomes

Exosomes from both ticagrelor-pretreated and untreated H9c2 cardiomyocytes were characterized with flow cytometry (Fig. 2A) and evaluated using the Tunable Resistive Pulse Sensing (TRPS) technology by qNanoGold. Size ranges of exosomes were similar in both groups with an approximate size range of 65–240 nm (Fig. 2B). Also, we confirmed the exosome uptake of H9c2 cardiomyocytes with DiI-staining (Fig. 2C).

Ticagrelor-pretreatment modulates the angiogenic and migrates properties of H9c2-derived exosomes

We, first, have evaluated the functional effects of ticagrelor pretreatment on the modulation of H9c2 derived exosomes. For this purpose, HUVECs were treated with either ticagrelor-pretreated or untreated H9c2 derived exosomes. The changes in the angiogenic and migration ability of HUVEC upon exosomes treatment were investigated by tube formation and wound healing assay. As can be seen in Figure 3A, ticagrelor-pretreatment induced H9c2-exosomes caused a significant increase in branches, mesh, segment, and node formation of HUVECs at the 6th and 24th hours of incubation (Fig. 3B). Ticagrelor-pretreatment also enhanced the release of exosomes from H9c2 cells that directly contribute to endothelial cell migration (Fig. 4A and 4B)

Ticagrelor-pretreated H9c2-derived exosomes provide a direct beneficial effect on ROS production in HG cardiomyocytes.

In a previous study, it was demonstrated that ticagrelor-treatment markedly prevents the aberrant ROS production in insülin-resistant H9c2 cells [18]. Here we evaluated the alteration of ROS production of HG cardiomyocytes depending on the ticagrelor induced H9c2 exosome treatment. The response of HG cells to H_2O_2 is calculated by a change in fluorescence intensity to represent ROS level at the cellular level. ROS level of HG cardiomyocytes was significantly higher than control cardiomyocytes ($p<0.001$). As shown in Figure 5A, HG cardiomyocytes incubated with control H9c2-exosomes showed similar ROS levels compare to un-treated HG cardiomyocytes, indicating control exosomes do not affect oxidative stress. However, administration of ticagrelor-pretreated exosomes caused a significant decrease in the enhanced ROS production level in HG cardiomyocytes.

Ticagrelor-pretreated H9c2-derived exosomes suppress expression levels of apoptosis and ER-stress markers in HG cardiomyocytes

Treatment of HG cardiomyocytes with released exosomes from ticagrelor-pretreated H9c2 cells significantly prevented the increased level of apoptosis (Fig. 5B). Exosomes in ticagrelor-pretreated HG-H9c2 significantly attenuated the expression levels of ER stress markers. The mRNA level of GRP78 was approximately 2-fold lower in HG cardiomyocytes treated with ticagrelor induced H9c2-exosomes comparing to untreated H9c2-exosomes treated HG cells (Fig. 5C). Similarly, the enhanced level of

another ER stress marker calregulin was reversed following the administration of ticagrelor-pretreated exosomes (Fig. 5D).

Ticagrelor induced H9c2 exosomes inhibits the expression of autophagy markers in HG cardiomyocytes

As shown in Figure 6, treatment of HG cardiomyocytes with exosomes derived from ticagrelor included H9c2 cells causes the inhibition of the expression of autophagy markers Bnip3 (Fig. 6A), equilibrative nucleoside transporter ENT1 (Fig. 6B), and Beclin (Fig. 6C), which is drastically upregulated depending on the hyperglycemia. Of note, the control-exosome treatment has shown any remarkable effect in induced autophagy formation in HG cardiomyocytes.

Ticagrelor induced H9c2-exosome upregulates the miR-499, miR-133a, and miR-133b in HG cardiomyocytes

We have also evaluated the changes in mRNA levels of oxidative stress and cardiomyopathy-related associated miRNAs at the cellular and exosomal level. It is well-known that miR-499, miR-133a, and miR-133b are tightly associated with a cardiac action potential, oxidative stress, apoptosis, and cardiomyopathy [19,20]. The significantly decreased expression levels of miR-499, miR-133a, and miR-133b in DM cardiomyocytes were also reported in the previous study [21]. First, we demonstrated that the downregulated expression of miR-499 (Fig. 6D), miR-133a (Fig. 6E), and miR-133b (Fig. 6F) in DM cardiomyocytes was drastically reversed following the ticagrelor-pretreated H9c2 exosome administration. In addition, to analyze the effect of ticagrelor on DM cardiomyocyte-derived exosomes, we have also investigated the changes in the expression level of exosomal miR-499, miR-133a, and miR-133b. Similar to the expressional changes in cellular miRNA level, exosomal miR-499, miR-133a, and miR-133b released from DM cardiomyocytes have shown a significant increase in the presence of ticagrelor comparing to untreated DM cardiomyocytes (Fig. 6G-I).

Next, to verify which biological processes, that are regulated by miR-499, miR-133a, and miR-133b, are associated with the pathogenesis of diabetic cardiomyopathy through miRNA-regulated mRNA dysregulation, GO terms and KEGG pathways enrichment analyses were performed. The 268 common genes were indicated which are the predicted targets of miR-499, miR-133a, and miR-133b. miRNA-mRNA regulatory network of these 268 common genes and four differentially miRNA was used to construct the Cytoscape (Fig. 7a). These 268 common genes and three differentially expressed miRNAs identified in our study were used to construct miRNA-mRNA regulatory network visualized in Cytoscape, which consisted of 386 nodes and 430 edges, including 386 overlapping genes. Among the 412 enriched categories, 20 of them were found to be significantly related to given miRNAs regulation, including mitotic cell cycle, regulation of cell cycle, tube morphogenesis, vasculature development, blood vessel development, blood vessel morphogenesis, apoptotic signaling pathway, response to hypoxia and endothelial cell migration.

GO enrichment analysis results showed that variations in the predicted targets of miR-499, miR-133a, and mir-133b linked with BP were mainly enriched in nitrogen compound metabolic process, cell death,

cellular response to stress, regulation of cell death (apoptosis, anoikis), cellular response to DNA damage stimulus, proteasome-mediated ubiquitin-dependent protein catabolic process, heart development, positive regulation of cell migration, response to wounding, endoplasmic reticulum organization, positive regulation of glucose metabolic process, and mitochondrial fragmentation involved in the apoptotic process (Fig. 7b).

Discussion

In the present study, we demonstrated an important action of ticagrelor, a drug directly targeting P_2Y_{12}-receptors, on cardiomyocytes-derived exosomes in hyperglycemic cardiomyocytes. Our present data further emphasized that ticagrelor exerts its regulatory effect on diabetic cardiomyopathy through exosomal modulation beyond its antiplatelet action. We demonstrated the importance of ticagrelor-pretreatment of cardiomyocytes to obtain the benefits of exosome modulation in heart functions under pathological conditions including diabetes in vitro.

Among long-term complications of DM, there are both macro-level and micro-level abnormalities, leading to heart diseases besides other complications. DM, at cellular levels, is associated with detectable changes in intracellular function and structure of cardiomyocytes through effecting several molecular mechanisms including oxidative stress, inflammation, apoptosis and autophagy, miRNA regulation, mitochondrial dysfunction, and ER stress [19–21]. Since DM is a major killer worldwide and its very rapid rise emphasizes a serious threat to humans, there are great efforts to develop novel therapeutic approaches for DM management [16, 17, 22].

DM patients have a high risk for cardiovascular disease, named diabetic cardiomyopathy. Diabetic cardiomyopathy, being a noticeably different pathology from heart failure, was first defined by Rubler and co-workers [23], which does not include coronary atherosclerosis but is characterized by an irreversible loss of cardiomyocytes, the contractile cellular units of the heart. Over the last two decades, studies focused on stem cell therapy as a potential approach for cardiac repair [24] and it is observed that a large part of the benefit of the injection of stem and progenitor cells into injured hearts is mediated by secreted factors [25]. The study by Wang et al. [26] advances our understanding of the role of cardiomyocyte exosomes and hints at the complexity of exosomal cargo under diabetic conditions. Here, for the first time in the literature, we have explored the role of ticagrelor-pretreatment of H9c2 myocardium cells, and then on the degree of beneficial effects of exosomes derived from them.

Although it was reported that ticagrelor administration blockades tumor angiogenesis via suppressing inflammation [27,11], the increased co-localization of c-Kit protein, a marker of cardiac stem cells and CD31 protein, a marker of endothelial cells, around blood vessels upon ticagrelor treatment demonstrated the positive effect of ticagrelor on angiogenesis following myocardial ischemia-reperfusion in the rat [28]. Moreover, the increased levels of circulating endothelial progenitor cells in diabetic patients after ticagrelor administration were also reported [29]. Since the angiogenic contribution of the ticagrelor is

known, it is conceivable that ticagrelor may exert this effect via modulating the angiogenic properties of exosomes derived from ticagrelor-treated cardiomyocytes. We found- for the first time- that ticagrelor-pretreatment markedly induces branche, mesh, segment, and node formation of HUVECs at the 6th and 24th hours of incubation. Endothelial cells are more susceptible to hyperglycemia-induced damage than other cell types [30]. Diabetes causes endothelial dysfunction through the impairment of several mechanisms, including oxidative stress, inflammatory activation and increased permeability of the endothelial cell layer in the myocardium, and decreased capillary density [31,32]. Hyperglycemia-mediated activation of the diacylglycerol (DAG)-PKC signaling pathway is involved in the induction of oxidative stress excessive production of free radicals, which in turn promote endothelial dysfunction which leads to diabetic cardiomyopathy [31,33]. Through the above results, endothelial cells may be considered as a potential therapeutic target in the treatment of diabetes. Here, we have also demonstrated that exosomes released from H9c2 cells pretreated with 1-μM ticagrelor significantly increase endothelial cell migration. Considering that under hyperglycemic conditions, endothelial cell viability and migration reduces, our findings could provide that ticagrelor-pretreatment reverses endothelial dysfunction in an exosome-mediated paracrine manner.

It is well established that ticagrelor therapy administered in diabetic patients demonstrated a direct beneficial effect against heart dysfunction beyond its antiplatelet action [34,35]. Olgar et al reported that ticagrelor provided a significant improvement in mitochondrial membrane potential, a marked decrease in cellular ROS production, a normalization of the increased resting level of cytosolic Ca^{2+}, and preservation of cellular ATP production. Moreover, in that study, it was also demonstrated that ticagrelor alleviates enhanced ER stress, autophagosomes formation, and apoptosis by inhibiting the expression of the genes involved in these molecular pathways [18]. However, the exact subcellular mechanisms by which ticagrelor exerts its cardioprotective, anti-hypoxic, and anti-apoptotic effect remains to be elucidated. Consistently, Casiere and co-workers have shown that long-term treatment with the lower dose of ticagrelor enhances anti-hypoxic and anti-apoptotic effects of exosomes released from human cardiac-derived mesenchymal progenitor cells (hCPC) via attenuating the increase of HIF1α levels in hypoxic cardiomyocytes [16]. This finding revealed the new role of ticagrelor in the regulation of anti-apoptotic and anti-hypoxic properties of exosomes derived from hCPCs, which are stem/progenitor cells resident in the adult heart [36]. Taken into consideration the well-established actions of ticagrelor, particularly, associated with exosomal modulation in terms of cardiac regeneration and cardiomyocyte death, in this study, we have demonstrated that ticagrelor induced H9c2 exosomes have a direct beneficial effect on hyperglycemic ventricular cardiomyocyte causing a marked decrease in cellular ROS production.

Superoxide production is also associated with ENT1, while ENT1 plays a central role in the determination of the extracellular content of adenosine, which is generated extracellularly by the degradation of ATP [37]. Upon ischemic reperfusion, ENT1 directly involves the formation of superoxide radicals [38] and plays an essential role in cardioprotection via modulating purine nucleoside-dependent signaling in the heart [18,39]. Taken together, our data revealed that ticagrelor exerts its cardioprotective effect on oxidative stress-associated several factors through exosomal modulation.

Diabetic cardiomyopathy can be a major cause of diabetes-related mortality. Emerging preclinical and clinical evidence demonstrates that diabetes induces cardiomyocyte apoptosis. On the other hand, cardiac autophagy is still a controversial issue. In addition to the beneficial effect of autophagy during ischemic reperfusion [40], uncontrolled excessive induction of autophagy may contribute to autophagic cardiomyocyte death [41]. Bcl-2 family members Bnip3 and Beclin are key regulators of necrosis, autophagy, and/or apoptosis [42]. Consistent with the previous study [18] our data demonstrated treatment of HG cardiomyocytes with exosomes derived from ticagrelor included H9c2 cells causes the inhibition of the expression of autophagy and apoptosis markers, which are drastically upregulated depending on the hyperglycemia. Of note, the control-exosome treatment has shown a remarkable effect in induced autophagy formation and apoptosis in HG cardiomyocytes.

Furthermore, it is also well accepted that autophagy was induced as an adaptive response against ER stress since it was sensitive to ER-stress inhibition [43]. Supporting these statements, it was reported that ticagrelor can directly affect cardiomyocytes and provide marked protection against ER stress and dramatic induction of autophagosomes, and therefore, can alleviate the ER stress-induced increases in oxidative stress and cell apoptosis during insulin resistance [18,44]. In the present study, we have shown that ticagrelor exerts this suppressive effect on markedly increased ER stress via modulating released exosomes from H9c2 cells which cause the significant downregulation of mRNA level of ER stress markers. Finally, we have also tested have also evaluated the changes in mRNA levels of oxidative stress and cardiomyopathy-related associated cellular and exosomal miRNAs. Previously, lipopolysaccharide-treated rat cardiomyocytes showed a marked decrease in expression of miR-499 that inhibited the expression of pro-apoptotic genes and upregulated expression of the anti-apoptotic gene *BCL-xL* by targeting *SOX6* and *PDCD4*, which play important roles in cardiac differentiation of P19CL6 cells [45] and the protection of cardiomyocytes against H2O2-induced injury [46], respectively. In a mouse diabetic cardiomyopathy model, Chen et al demonstrated that miR-133a, expressed in both skeletal and cardiac muscle, significantly decreased the expression of TGF-β1 signaling and increased the expression of acidic fibroblast growth factor1 (FGF1) that could induce ERK1/2 phosphorylation accompanied by enhanced production of extracellular matrix proteins, FN1 and COL4A1, hallmarks of cardiac fibrosis [47]. miR-133b, which is expressed specifically in skeletal muscle, was reported to be downregulated in STZ-induced diabetic rats concerning increased oxidative stress [21] and protected H9c2 against hypoxia injury via downregulation of nucleotide-binding oligomerization domain-like receptor protein 3 (NLRP3) [48]. Downregulated expression of cellular miR-499, miR-133a, and miR-133b in HG-cardiomyocytes associated with diabetes was drastically upregulated upon ticagrelor-induced H9c2 exosome treatment. Considering the important fact, a diabetic heart composes both healthy and diabetic cardiomyocytes, we have also examined the therapeutic paracrine effect of DM cardiomyocytes following the ticagrelor treatment. Exosomal miR-499, miR-133a, and miR-133b in hyperglycemic cardiomyocytes were upregulated upon ticagrelor treatment. These results supported that ticagrelor treatment may promote the therapeutic effect of exosomes released from both healthy and hyperglycemic cardiomyocytes. In the current study, we have also examined predicted targets of miR-499, miR-133a, and miR-133b linked with

biological processes. biological and molecular functions, which are targets of miR-499, miR-133a, and miR-133b. These miRNAs have been involved as negative regulators in the pathway of apoptosis, positive regulators of cell migration, and wound healing, and cellular stress response. Such biological relevance of target genes elucidated through GO-enrichment may account for the pathogenesis in DCM through their involvement especially in heart development (GO:0007507) and positive regulation of glucose metabolic process (GO:0010907) ($p < 0.05$). Taken together, this analysis supports the effect of ticagrelor pretreatment on suppression of cellular stress, ROS production, cell death in addition to the contribution of angiogenesis and cell migration via modulation of exosomal profile.

Conclusions

Considering widely usage of ticagrelor for clinical therapy, these observations will get a special interest for clinicians to treat patients suffering from cardiac diseases associated with these cellular abnormalities. Our data reveal an unexpected regulatory mechanism of P_2Y_{12}- receptor antagonist, ticagrelor. Here we indicated the regulatory role of exosomes secreted by ventricular cardiomyocytes, possibly depending on induction of ticagrelor on the anti-hypoxic and anti-apoptotic signaling pathways in diabetic cardiomyopathy. We assume that elucidating the mechanisms of cardiometabolic drug actions on the complex signaling pathways may provide a promising alternative pharmacological usage to protect the heart against any pathological stimuli.

Limitation Of The Study

The major limitation of the study is that no in vivo data were presented to show the therapeutic effect of ticagrelor via regulating paracrine signaling of cardiomyocytes in the diabetic rat. In our study, we did not investigate the changes in exosomal miRNA profile depending on the ticagrelor treatment. The alteration of exosomal miRNA content, in terms of the cardioprotection, may support the present results and may reveal the potential targets of ticagrelor in exosome-based cardiomyocyte protection. However, further experiments focusing on the miRNA repertoire should be performed to confirm our *in vitro* results supporting wide evidence of ticagrelor-mediated cardioprotection.

Declarations

Data availability

Data is available from the authors by request.

Informed consent

Not applicable.

Conflict of interest

The authors declare that they have no competing interests.

Acknowledgments

This work was supported by grants Ankara University *Scientific Research Project* (*BAP*) Coordination Unit, Ankara, Turkey.

Author contributions

BT designed and supervised the research and provided the final approval of the version to be published. C.V.B, KCA, and B.T contributed to the study concept and design. C.V.B, Z.B.O., D.A., and K.G contributed and performed the experiments and analyzed the data. D.A. performed bioinformatical analysis. K.C.A supervised the research and contributed to the editing of the manuscript. S.D contributed to the manuscript writing. All authors critically revised the manuscript and approved the submitted version.

References

1. Davidson, S. M., Andreadou, I., Garcia-Dorado, D. & Hausenloy, D. J. Shining the spotlight on cardioprotection: beyond the cardiomyocyte. *Cardiovasc. Res*, **115**, 1115–1116 (2019).
2. Rosano, G. M., Vitale, C. & Seferovic, P. Heart Failure in Patients with Diabetes Mellitus. *Card. Fail. Rev*, **3**, 52–55 (2017).
3. Chung, S. M. *et al.* The Risk of Diabetes on Clinical Outcomes in Patients with Coronavirus Disease 2019: A Retrospective Cohort Study. *Diabetes Metab. J*, **44**, 405–413 (2020).
4. LaRocca, T. J., Sosunov, S. A., Shakerley, N. L., Ten, V. S. & Ratner, A. J. Hyperglycemic Conditions Prime Cells for RIP1-dependent Necroptosis *. *J. Biol. Chem*, **291**, 13753–13761 (2016).
5. Vilahur, G. *et al.* Polyphenol-enriched diet prevents coronary endothelial dysfunction by activating the Akt/eNOS pathway. *Rev. Esp. Cardiol. (Engl. Ed)*, **68**, 216–225 (2015).
6. Wernly, B., Erlinge, D., Pernow, J. & Zhou, Z. Ticagrelor: a cardiometabolic drug targeting erythrocyte-mediated purinergic signaling? *Am. J. Physiol. Heart Circ. Physiol*, **320**, H90–H94 (2021).
7. Mehta, S. R. *et al.* Effects of pretreatment with clopidogrel and aspirin followed by long-term therapy in patients undergoing percutaneous coronary intervention: the PCI-CURE study. *Lancet (London, England)*, **358**, 527–533 (2001).
8. Fu, S. *et al.* Extracellular vesicles in cardiovascular diseases. *Cell Death Discov*, **6**, 68 (2020).
9. Schober, A., Nazari-Jahantigh, M. & Weber, C. MicroRNA-mediated mechanisms of the cellular stress response in atherosclerosis. *Nature reviews. Cardiology*, **13**, 120 (2016).
10. Liu, Y. *et al.* Atherosclerotic Conditions Promote the Packaging of Functional MicroRNA-92a-3p Into Endothelial Microvesicles. *Circ. Res*, **124**, 575–587 (2019).
11. Li, H. *et al.* Coronary Serum Exosomes Derived from Patients with Myocardial Ischemia Regulate Angiogenesis through the miR-939-mediated Nitric Oxide Signaling Pathway. *Theranostics*, **8**, 2079–2093 (2018).

12. Singla, R., Garner, K. H., Samsam, M., Cheng, Z. & Singla, D. K. Exosomes derived from cardiac parasympathetic ganglionic neurons inhibit apoptosis in hyperglycemic cardiomyoblasts. *Mol. Cell. Biochem*, **462**, 1–10 (2019).
13. da Silva Novaes, A. *et al.* Influence of high glucose on mesangial cell-derived exosome composition, secretion and cell communication. *Sci. Rep*, **9**, 6270 (2019).
14. Saem, J. H. *et al.* Comparison of Ticagrelor Versus Prasugrel for Inflammation, Vascular Function, and Circulating Endothelial Progenitor Cells in Diabetic Patients With Non–ST-Segment Elevation Acute Coronary Syndrome Requiring Coronary Stenting. *JACC Cardiovasc. Interv*, **10**, 1646–1658 (2017).
15. Aït Mokhtar, O. *et al.* Pleiotropic effects of ticagrelor: Myth or reality? *Arch. Cardiovasc. Dis*, **109**, 445–448 (2016).
16. Casieri, V. *et al.* Ticagrelor Enhances Release of Anti-Hypoxic Cardiac Progenitor Cell-Derived Exosomes Through Increasing Cell Proliferation In Vitro. *Sci. Rep*, **10**, 2494 (2020).
17. He, Q. *et al.* Mesenchymal stem cell-derived exosomes exert ameliorative effects in type 2 diabetes by improving hepatic glucose and lipid metabolism via enhancing autophagy. *Stem Cell Res. Ther*, **11**, 223 (2020).
18. Olgar, Y. *et al.* Ticagrelor reverses the mitochondrial dysfunction through preventing accumulated autophagosomes-dependent apoptosis and ER stress in insulin-resistant H9c2 myocytes. *Mol. Cell. Biochem*, **469**, 97–107 (2020).
19. Xiao, Y., Zhao, J., Tuazon, J. P., Borlongan, C. V. & Yu, G. MicroRNA-133a and Myocardial Infarction. *Cell Transplant*, **28**, 831–838 (2019).
20. Huang, J. H., Xu, Y., Yin, X. M. & Lin, F. Y. Exosomes Derived from miR-126-modified MSCs Promote Angiogenesis and Neurogenesis and Attenuate Apoptosis after Spinal Cord Injury in Rats., **424**, 133–145 (2020).
21. Yildirim, S. S., Akman, D., Catalucci, D. & Turan, B. Relationship between downregulation of miRNAs and increase of oxidative stress in the development of diabetic cardiac dysfunction: junctin as a target protein of miR-1. *Cell Biochem. Biophys*, **67**, 1397–1408 (2013).
22. 9. Pharmacologic Approaches to Glycemic Treatment: Standards of Medical Care in Diabetes-2021., **44**, S111–S124 (2021).
23. Rubler, S. *et al.* New type of cardiomyopathy associated with diabetic glomerulosclerosis. *Am. J. Cardiol*, **30**, 595–602 (1972).
24. Nguyen, P. K., Rhee, J. W. & Wu, J. C. Adult Stem Cell Therapy and Heart Failure, 2000 to 2016: A Systematic Review. *JAMA Cardiol*, **1**, 831–841 (2016).
25. He, N., Zhang, Y., Zhang, S., Wang, D. & Ye, H. Exosomes: Cell-Free Therapy for Cardiovascular Diseases. *J. Cardiovasc. Transl. Res*, **13**, 713–721 (2020).
26. Wang, X. *et al.* Hsp20-Mediated Activation of Exosome Biogenesis in Cardiomyocytes Improves Cardiac Function and Angiogenesis in Diabetic Mice., **65**, 3111–3128 (2016).

27. Mitrugno, A. & McCarty, O. J. T. Ticagrelor breaks up the tumor-platelet party., **130**, 1177–1178 (2017).
28. Birnbaum, Y. *et al.* Ticagrelor improves remodeling, reduces apoptosis, inflammation and fibrosis and increases the number of progenitor stem cells after myocardial infarction in a rat model of ischemia reperfusion. *Cell. Physiol. Biochem*, **53**, 961–981 (2019).
29. Jeong, H. S. *et al.* Comparison of Ticagrelor Versus Prasugrel for Inflammation, Vascular Function, and Circulating Endothelial Progenitor Cells in Diabetic Patients With Non–ST-Segment Elevation Acute Coronary Syndrome Requiring Coronary Stenting: A Prospective, Randomized. *JACC Cardiovasc. Interv*, **10**, 1646–1658 (2017).
30. Knapp, M., Tu, X. & Wu, R. Vascular endothelial dysfunction, a major mediator in diabetic cardiomyopathy. *Acta Pharmacol. Sin*, **40**, 1–8 (2019).
31. Haidari, M., Zhang, W., Willerson, J. T. & Dixon, R. A. Disruption of endothelial adherens junctions by high glucose is mediated by protein kinase C-β-dependent vascular endothelial cadherin tyrosine phosphorylation. *Cardiovasc. Diabetol*, **13**, 105 (2014).
32. Viberti, G. C. Increased capillary permeability in diabetes mellitus and its relationship to microvascular angiopathy. *Am. J. Med*, **75**, 81–84 (1983).
33. Yuan, S. Y. *et al.* Protein kinase C activation contributes to microvascular barrier dysfunction in the heart at early stages of diabetes. *Circ. Res*, **87**, 412–417 (2000).
34. Yang, H., Tang, B., Xu, C. H. & Ahmed, A. Ticagrelor Versus Prasugrel for the Treatment of Patients with Type 2 Diabetes Mellitus Following Percutaneous Coronary Intervention: A Systematic Review and Meta-Analysis. *Diabetes Ther*, **10**, 81–93 (2019).
35. Sweeny, J. M. *et al.* Impact of Diabetes Mellitus on the Pharmacodynamic Effects of Ticagrelor Versus Clopidogrel in Troponin-Negative Acute Coronary Syndrome Patients Undergoing Ad Hoc Percutaneous Coronary Intervention. *J. Am. Heart Assoc*, **6**, e005650 (2017).
36. Barile, L., Moccetti, T., Marbán, E. & Vassalli, G. Roles of exosomes in cardioprotection. *Eur. Heart J*, **38**, 1372–1379 (2017).
37. Mikdar, M. *et al.* The equilibrative nucleoside transporter ENT1 is critical for nucleotide homeostasis and optimal erythropoiesis., **137**, 3548–3562 (2021).
38. Abd-Elfattah, A. S., Aly, H., Hanan, S. & Wechsler, A. S. Myocardial protection in beating heart cardiac surgery: I: pre- or postconditioning with inhibition of es-ENT1 nucleoside transporter and adenosine deaminase attenuates post-MI reperfusion-mediated ventricular fibrillation and regional contractile dysfunc. *J. Thorac. Cardiovasc. Surg*, **144**, 250–255 (2012).
39. Rose, J. B. *et al.* Equilibrative nucleoside transporter 1 plays an essential role in cardioprotection. *Am. J. Physiol. - Hear. Circ. Physiol*, **298**, 771–777 (2010).
40. Ma, S., Wang, Y., Chen, Y. & Cao, F. The role of the autophagy in myocardial ischemia/reperfusion injury. *Biochim. Biophys. Acta - Mol. Basis Dis*, **1852**, 271–276 (2015).
41. Valentim, L. *et al.* Urocortin inhibits Beclin1-mediated autophagic cell death in cardiac myocytes exposed to ischaemia/reperfusion injury. *J. Mol. Cell. Cardiol*, **40**, 846–852 (2006).

42. Burton, T. R. & Gibson, S. B. The role of Bcl-2 family member BNIP3 in cell death and disease: NIPping at the heels of cell death. *Cell Death Differ*, **16**, 515–523 (2009).
43. Park, M., Sabetski, A., Kwan Chan, Y., Turdi, S. & Sweeney, G. Palmitate induces ER stress and autophagy in H9c2 cells: implications for apoptosis and adiponectin resistance. *J. Cell. Physiol*, **230**, 630–639 (2015).
44. Wang, X. *et al.* Beneficial effect of ticagrelor on microvascular perfusion in patients with ST-segment elevation myocardial infarction undergoing a primary percutaneous coronary intervention. *Coron. Artery Dis*, **30**, 317–322 (2019).
45. Li, X. *et al.* MiR-499 regulates cell proliferation and apoptosis during late-stage cardiac differentiation via Sox6 and cyclin D1. *PLoS One*, **8**, e74504 (2013).
46. Wang, J. *et al.* miR-499 protects cardiomyocytes from H 2O 2-induced apoptosis via its effects on Pdcd4 and Pacs2. *RNA Biol*, **11**, 339–350 (2014).
47. Chen, S. *et al.* Cardiac miR-133a overexpression prevents early cardiac fibrosis in diabetes. *J. Cell. Mol. Med*, **18**, 415–421 (2014).
48. Zhou, Y., Huang, H. & Hou, X. MicroRNA-133b Alleviates Hypoxia Injury by Direct Targeting on NOD-Like Receptor Protein 3 in Rat H9c2 Cardiomyocyte. Cardiol. Res. Pract. 2019, 8092461 (2019).
49. Kornilov, R. *et al.* Efficient ultrafiltration-based protocol to deplete extracellular vesicles from fetal bovine serum. *J. Extracell. vesicles*, **7**, 1422674 (2018).
50. Liang, C. C., Park, A. Y. & Guan, J. L. In vitro scratch assay: a convenient and inexpensive method for analysis of cell migration in vitro. *Nat. Protoc*, **2**, 329–333 (2007).
51. Suarez-Arnedo, A. *et al.* An image J plugin for the high throughput image analysis of in vitro scratch wound healing assays. *PLoS One*, **15**, e0232565–e0232565 (2020).
52. Jabbari, N., Nawaz, M. & Rezaie, J. Bystander effects of ionizing radiation: conditioned media from X-ray irradiated MCF-7 cells increases the angiogenic ability of endothelial cells. *Cell Commun. Signal*, **17**, 165 (2019).
53. Carpentier, G. *et al.* Angiogenesis Analyzer for ImageJ — A comparative morphometric analysis of “Endothelial Tube Formation Assay” and “Fibrin Bead Assay”. *Sci. Rep*, **10**, 11568 (2020).
54. Tuncay, E. *et al.* Zn2+-transporters ZIP7 and ZnT7 play important role in progression of cardiac dysfunction via affecting sarco(endo)plasmic reticulum-mitochondria coupling in hyperglycemic cardiomyocytes., **44**, 41–52 (2019).
55. Chen, C. *et al.* Real-time quantification of microRNAs by stem-loop RT-PCR. *Nucleic Acids Res*, **33**, e179 (2005).
56. Kramer, M. F. Stem-loop RT-qPCR for miRNAs. Curr. Protoc. Mol. Biol. Chapter 15, Unit 15.10(2011).
57. Ritchie, M. E. *et al.* Empirical array quality weights in the analysis of microarray data. *BMC Bioinformatics*, **7**, 261 (2006).
58. 2019, R. K. P. P. H. R. P. V. 1. 012.No Title.

59. Https://doi.org/10.1007/978-0-387-98141-3, W. H. (2009). Ggplot2: Elegant Graphics for Data Analysis. *Ggplot2 Elegant Graph. Data Anal.*
60. Slowikowski, K. No Title. Get. started with ggrepel(2021).
61. Dweep, H. & Gretz, N. miRWalk2.0: a comprehensive atlas of microRNA-target interactions. *Nature methods*, **12**, 697 (2015).
62. Chen, Y. & Wang, X. miRDB: an online database for prediction of functional microRNA targets. *Nucleic Acids Res*, **48**, D127–D131 (2020).
63. Garcia, D. M. *et al.* Weak seed-pairing stability and high target-site abundance decrease the proficiency of lsy-6 and other microRNAs. *Nat. Struct. Mol. Biol*, **18**, 1139–1146 (2011).
64. Paraskevopoulou, M. D. *et al.* DIANA-microT web server v5.0: service integration into miRNA functional analysis workflows. *Nucleic Acids Res*, **41**, W169–73 (2013).
65. Bindea, G. *et al.* ClueGO: a Cytoscape plug-in to decipher functionally grouped gene ontology and pathway annotation networks., **25**, 1091–1093 (2009).

Figures

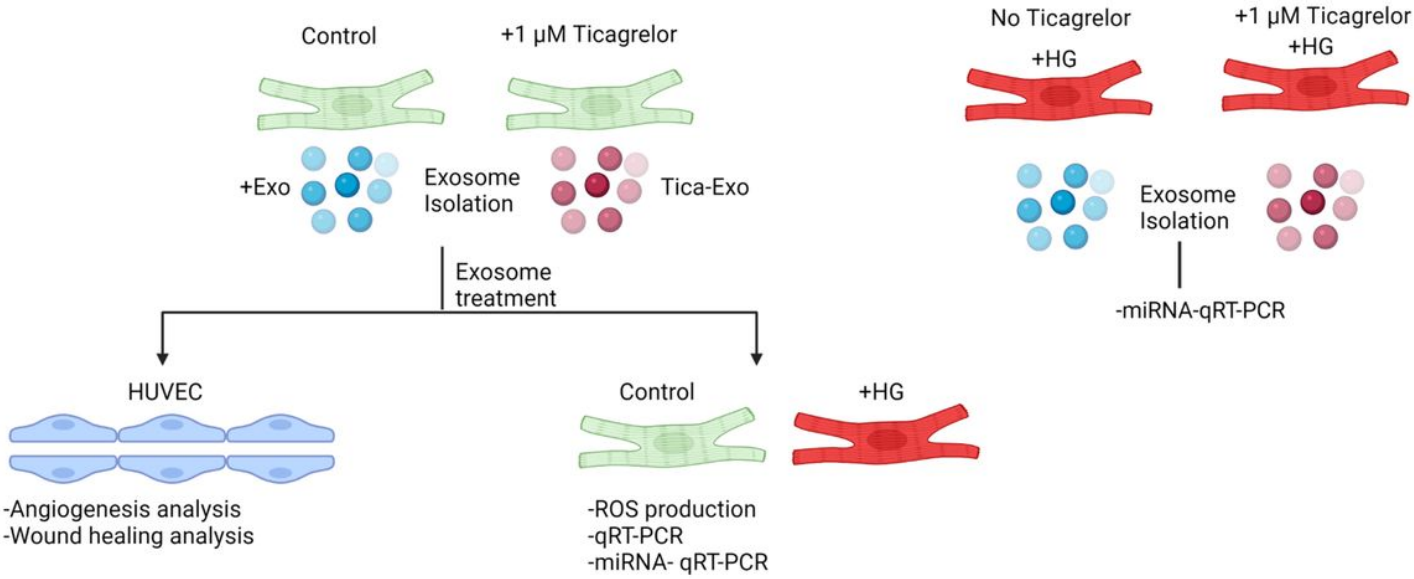

Figure 1

The experimental model used and protocols followed in the present study. The Diabetes model was mimicked using the H9c2 cell line. Exosomes derived from ticagrelor treated and untreated H9c2 cells were analyzed at the functional and molecular levels.

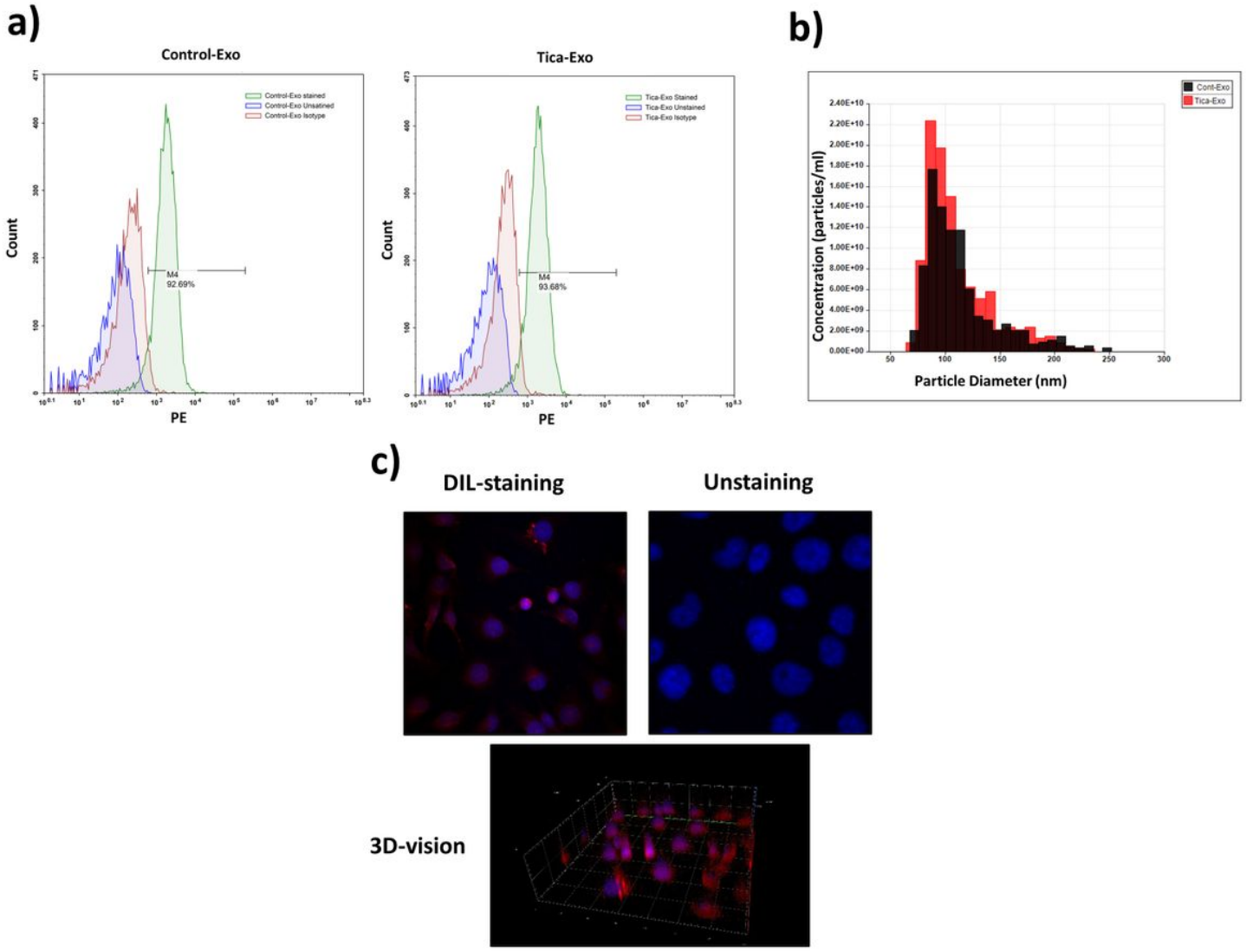

Figure 2

Characterization and quantification of isolated exosomes. (a) Flow cytometric analysis was performed using magnetic beads coated with CD9 exosome marker. These coated beads were incubated with a PE-conjugated CD81 antibody. IgG Isotype control was used. M4 shows the percentage of PE-positive beads. (b) Size distribution and quantification of isolated extracellular vesicles were analyzed using qNanoGold. For exosome samples, a polyurethane nanopore rated for particles <100 nm (NP100-, Izon Science, UK) was used. The measured mean diameter of exosomes was approximately 100 nm. (c) The uptake of DiI-labeled exosomes by H9c2 cells was visualized by confocal microscopy

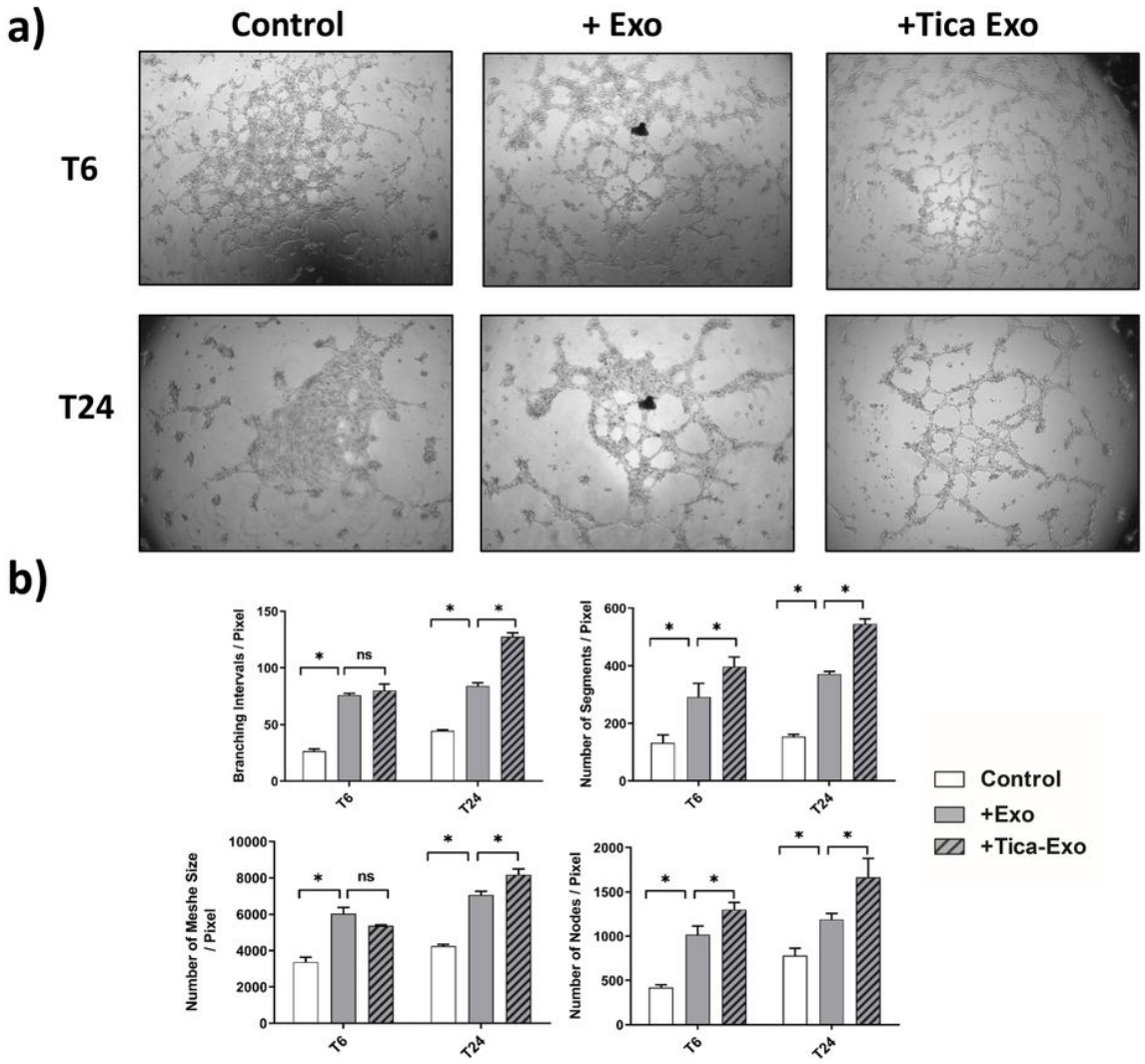

Figure 3

Effects of ticagrelor (Tica, 1 μM) pretreated H9c2-derived exosome (+Tica-Exo) on angiogenesis were evaluated by angiogenesis assay using Matrigel. (a) The HUVEC cells were seeded on matrigel and incubated either with control (+Exo) or ticagrelor-pretreated H9c2-derived exosomes (Tica-Exo). Representative images show that TicaExo treatment causes a marked increase in vasculogenesis. (b) The changes in branches, mesh, segment, and node formation of HUVECs at the 6th h and 24th h of incubation were analyzed by ImageJ. Data are expressed as the mean±SD (n=3). *P<0.05, n.s: not significant.

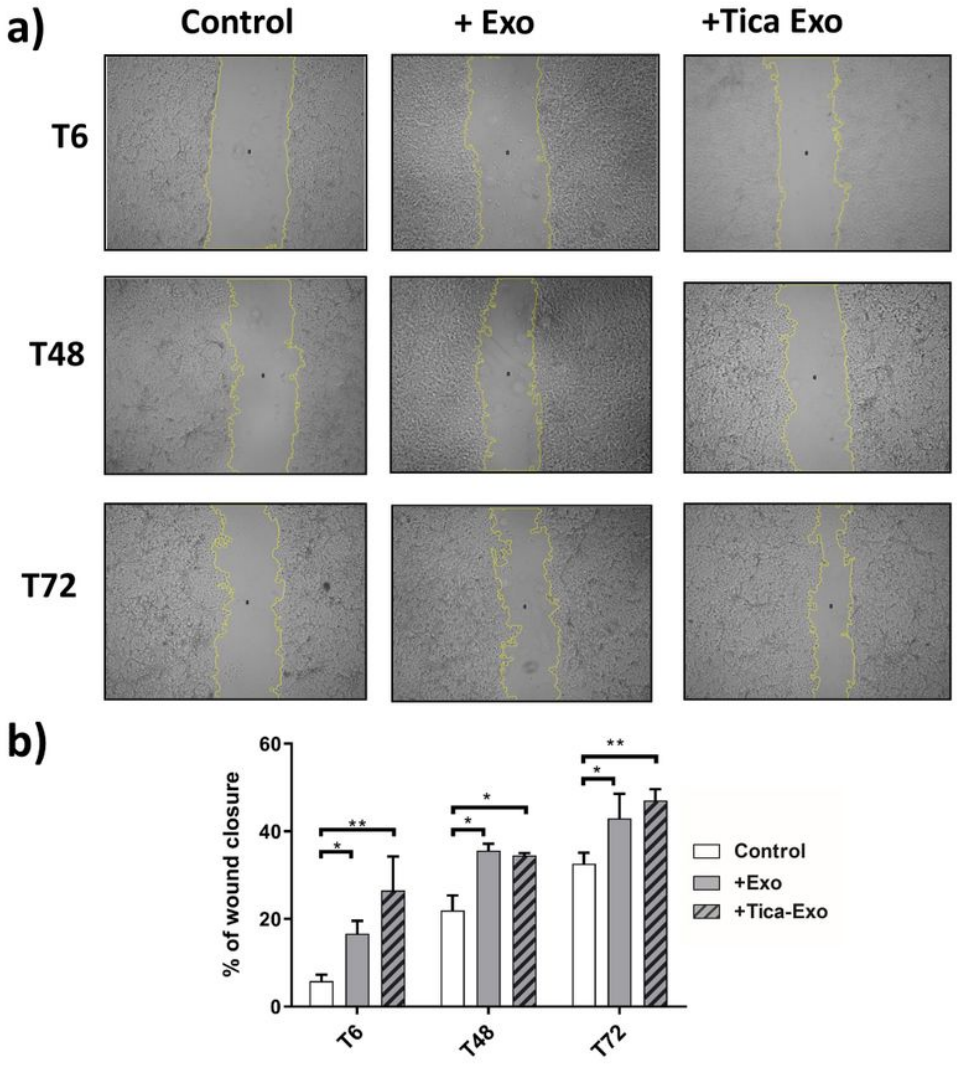

Figure 4

Effects of ticagrelor (Tica, 1-μM) pretreated H9c2-derived exosome (+Tica-Exo) on cell migration by wound healing analysis. (a) The HUVEC cells were seeded on a 6-well plate and incubated either with control (+Exo) or ticagrelor-pretreated H9c2-derived exosomes (Tica-Exo). Representative images show that Tica-Exo treatment causes a significant increase in wound closure (b) The percentage of wound closure is analyzed by ImageJ and 6th h, 48th h, and 72nd h of incubation. Data are expressed as the mean±SD (n=3). *P<0.05, **P<0.01, n.s: not significant.

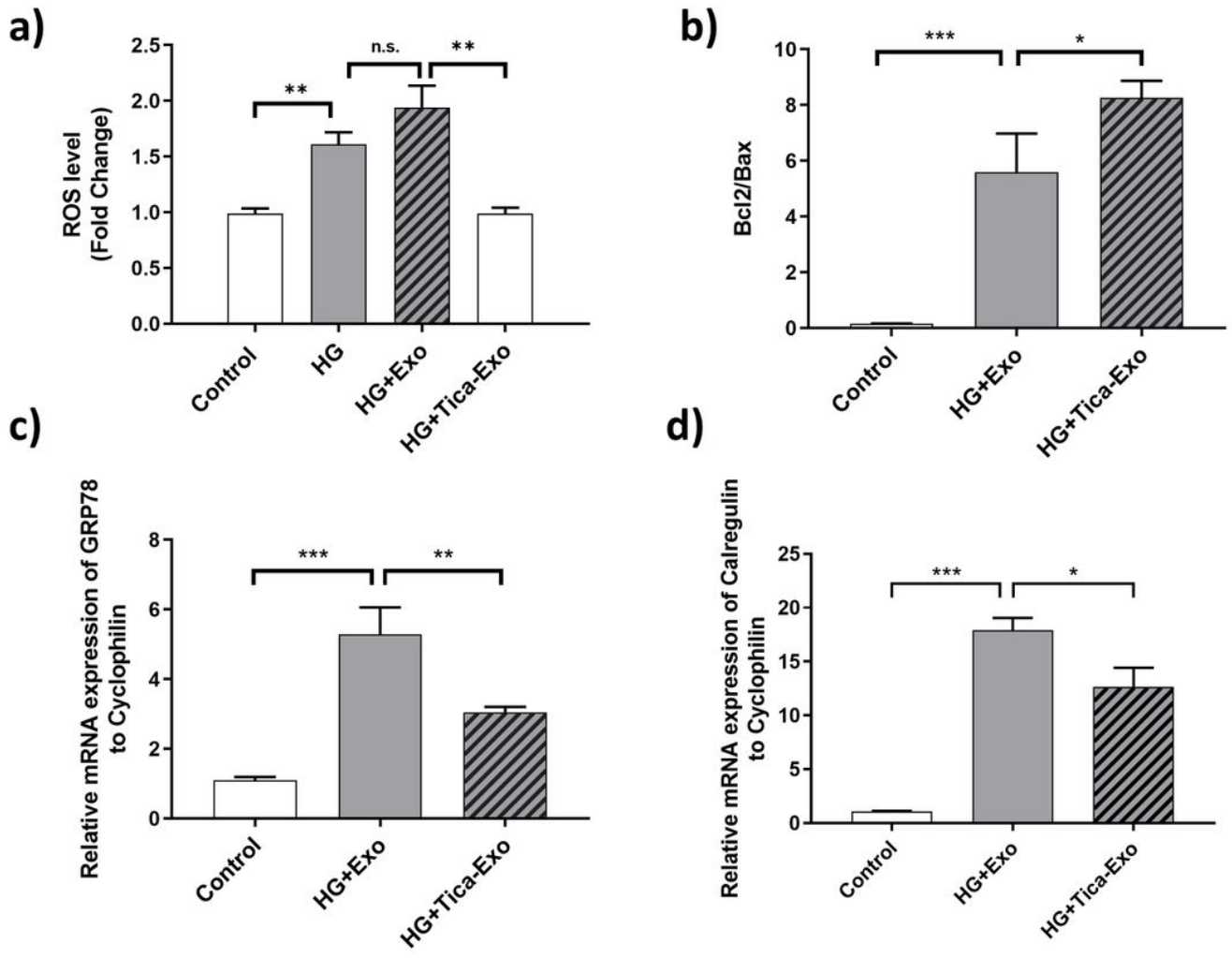

Figure 5

Effects of ticagrelor (Tica, 1-μM) pretreatment of oxidative stress and apoptosis markers. (a) The level of ROS production at the cellular level is measured in H9c2 cardiomyocytes. Ticagrelor-pretreated exosomes cause a significant decrease in the enhanced ROS production level in HG cardiomyocytes. (b) The mRNA expression of Bcl2 and Bax genes are analyzed by qRT-PCR. Bcl2/Bax ratio is induced upon ticagrelor-pretreated H9c2 exosome incubation in HG-incubated H9C2 cells. (c) Ticagrelor-pretreated H9c2 exosome treatment reverses the highly increased level of two molecular chaperones; GRP78 and (d) Calregulin mRNA expressions in HG-H9c2 cells. Data are expressed as the mean±SD (n=4). *P<0.05, **P<0.01, n.s: not significant.

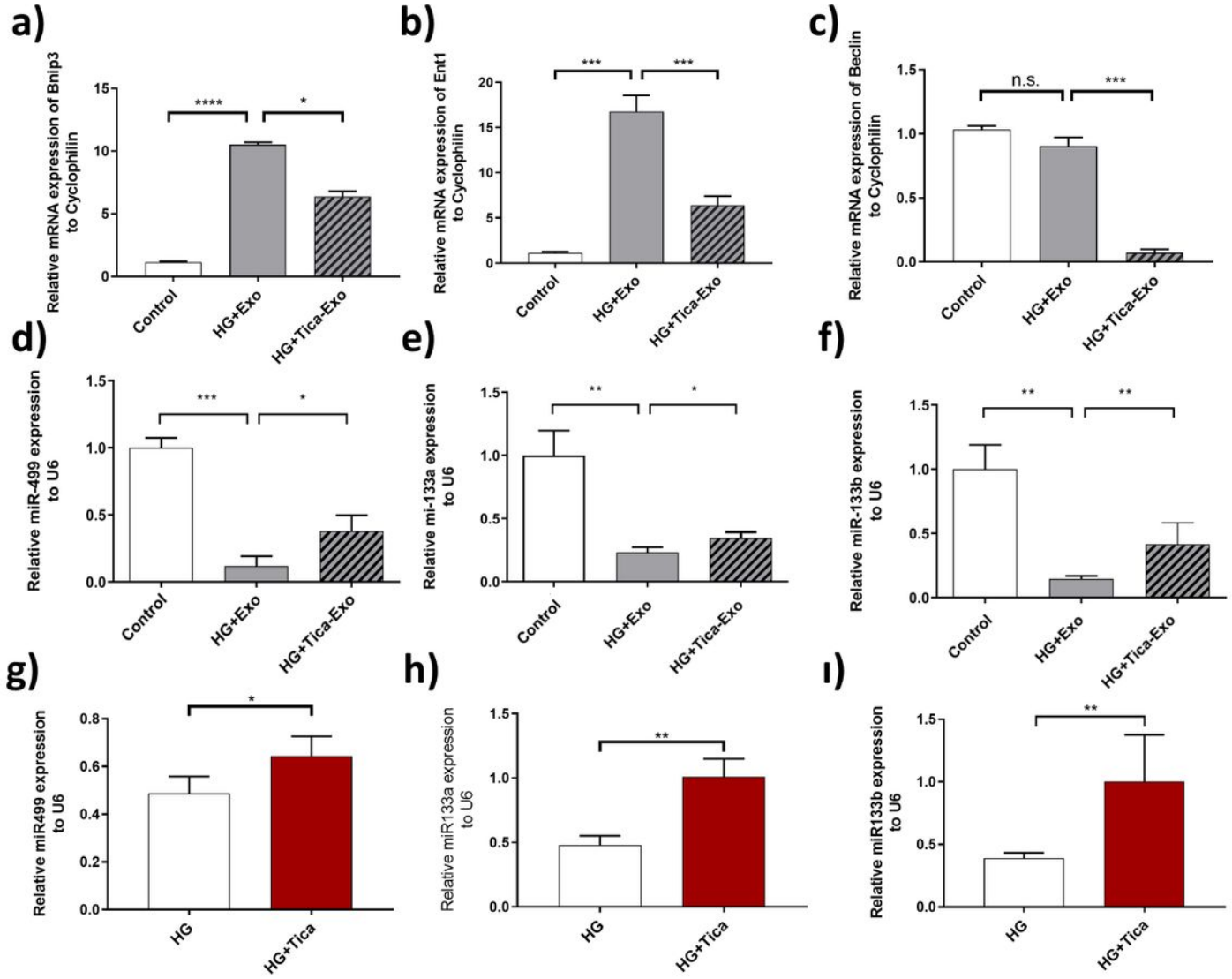

Figure 6

Effects of ticagrelor (Tica, 1 μM) pretreatment on autophagy markers and miRNA levels. The mRNA levels of autophagy regulator genes, evaluated by qRT-PCR in control and HG- H9c2 cells. Effects of ticagrelor-treated H9c2 exosomes on the mRNA levels of Bnip3 (a), Ent1(b), and Beclin (c) in HG-H9c2 cells comparing to control-Exo treated HG-H9c2 cells. The mRNA levels of cellular miR-499 (d), miR-133a (e), miR-133b (f). mRNA levels of exosomal miR-499 (g), miR-133a (h), miR-133b (ı) HG-H9c2 cells comparing to Exo treated HG-H9c2 cells. Data are expressed as the mean±SD (n=4). *P<0.05, **P<0.01, n.s: not significant.

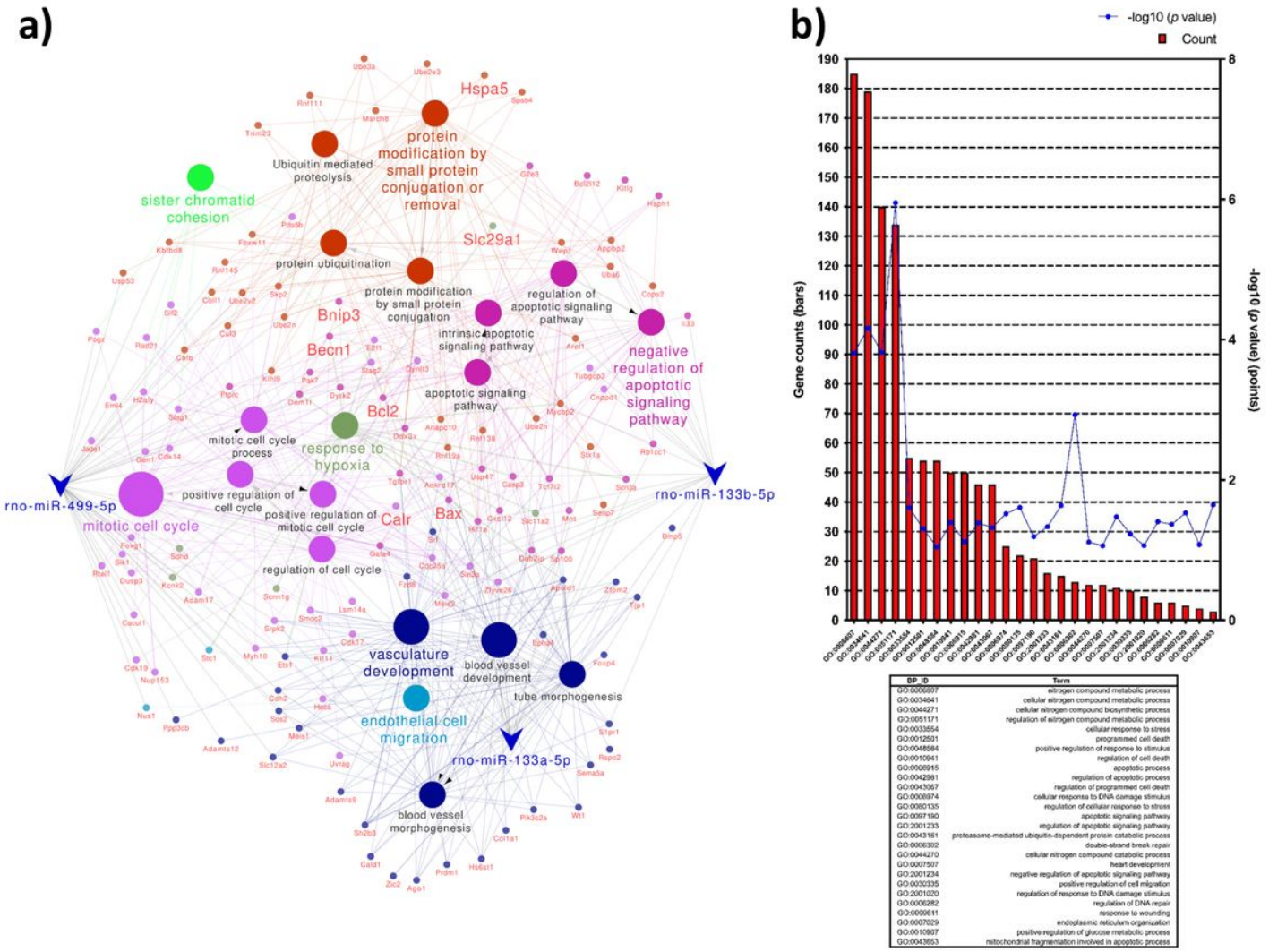

Figure 7

Verification of possible biological processes, regulated by the examined miRNAs associated with the pathogenesis of diabetic cardiomyopathy and representative GO-enriched functional annotations for the predicted targets of miRNAs from DAVID. a) The 268 common genes with predicted targets of rno-miR-499-5p, rno-miR-133a-5p and rno-miR-133b-5p were used to construct miRNA-mRNA regulatory network visualized in Cytoscape b) Database for Annotation, Visualization, and Integrated Discovery (DAVID; v6.8; https://david.ncifcrf.gov) online tool was used to determine the biological process (BP) attributes of GO for the candidate target genes of miR-499, miR-133a, and mir-133b. GO terms with modified Fisher exact p-value (EASE score) ≤ 0.1, FDR < 0.1, and N per group >3 were considered strongly enriched.

Supplementary Files

This is a list of supplementary files associated with this preprint. Click to download.

- SupplementaryTable1.docx

- SupplementaryTable2.docx
- RawDataGOandRanalysisdiyabeticCardiomyopathyGSE44179.xlsx